HHS Public Access

Author manuscript

J Control Release. Author manuscript; available in PMC 2020 October 01.

Published in final edited form as:

J Control Release. 2019 October ; 311-312: 201–211. doi:10.1016/j.jconrel.2019.09.001.

Creation of a Long-Acting Rilpivirine Prodrug Nanoformulation

James R. Hilaire[a], **Aditya N. Bade**[a], **Brady Sillman**[a], **Nagsen Gautam**[b], **Jonathan Herskovitz**[c], **Bhagya Laxmi Dyavar Shetty**[a], **Melinda S. Wojtkiewicz**[a], **Adam Szlachetka**[a], **Ben Lamberty**[a], **Sruthi Sravanam**[a], **Howard Fox**[a], **Yazen Alnouti**[b], **Prasanta K. Dash**[a], **JoEllyn M. McMillan**[a], **Benson J. Edagwa**[a,*], **Howard E. Gendelman**[a,b,*,‡]

[a]Department of Pharmacology and Experimental Neuroscience, University of Nebraska Medical Center, Omaha, NE 68198 USA

[b]Department of Pharmaceutical Sciences, University of Nebraska Medical Center, Omaha, NE 68198 USA

[c]Department of Pathology and Microbiology, University of Nebraska Medical Center, Omaha, NE 68198 USA

Abstract

Antiretroviral therapy requires lifelong daily dosing to attain viral suppression, restore immune function, and improve quality of life. As a treatment alternative, long-acting (LA) antiretrovirals can sustain therapeutic drug concentrations in blood for prolonged time periods. The success of recent clinical trials for LA parenteral cabotegravir and rilpivirine highlight the emergence of these new therapeutic options. Further optimization can improve dosing frequency, lower injection volumes, and facilitate drug-tissue distributions. To this end, we report the synthesis of a library of RPV prodrugs designed to sustain drug plasma concentrations and improved tissue biodistribution. The lead prodrug M3RPV was nanoformulated into the stable LA injectable NM3RPV. NM3RPV treatment led to RPV plasma concentrations above the protein-adjusted 90% inhibitory concentration for 25 weeks with substantial tissue depots after a single intramuscular injection in *BALB/cJ* mice. NM3RPV elicited 13- and 26-fold increases in the RPV apparent half-life and mean residence time compared to native drug formulation. Taken together, proof-of-concept is

[*]Corresponding authors: Howard E. Gendelman, M.D., Department of Pharmacology and Experimental Neuroscience, University of Nebraska Medical Center, Omaha, NE 68198-5880, USA; phone: 402-559-8920; fax: 402-559-3744; hegendel@unmc.edu and Benson J. Edagwa, Ph.D., Department of Pharmacology and Experimental Neuroscience, University of Nebraska Medical Center, Omaha, NE 68198-5800, USA; phone: 402-559-8916; fax: 402-559-7495; benson.edagwa@unmc.edu. [‡]Communication author (for submission and review): Howard E. Gendelman, M.D., Department of Pharmacology and Experimental Neuroscience, University of Nebraska Medical Center, Omaha, NE 68198-5880, USA; phone: 402-559-8920; fax: 402-559-3744; hegendel@unmc.edu.

Author Contributions

J.R.H. – design and execution of most experiments, data acquisition, data analysis, data interpretation, writing of manuscript. A.N.B. – design, execution, supervision of experiments, data interpretation and figure designs. B.S. – execution of experiments and data acquisition. N.G. – execution of experiments, data acquisition, data analysis. J.H. – design and execution of experiments. B.L.D.S. and M.W. – data acquisition and data analysis. A.S. – data acquisition. B.L. – data acquisition. S.S. – data acquisition. H.F. – study design. Y.A. – study design, data interpretation. P.K.D. – data acquisition and execution of experiments. J.M. – study design, supervision of experiments, data interpretation, data analysis. B.E. – conceived of the chemical drug synthesis and modifications, study design, supervision of experiments, data analysis and interpretation, writing of manuscript. H.E.G. – conceived the project, design of experiments, data interpretation, writing and editing of the manuscript and funding acquisition.

provided that nanoformulated RPV prodrugs can extend the apparent drug's half-life and improve tissue biodistribution. These results warrant further development for human use.

Keywords

Rilpivirine; Prodrugs; Antiretroviral therapy; Nanoformulation; Long-acting slow effective release antiretroviral therapy; Monocyte-derived macrophages

1. Introduction

Antiretroviral therapy (ART) has revolutionized the treatment of human immunodeficiency virus type one (HIV-1) infected people. Infection has evolved from certain death to a complete life free of most co-morbid conditions. Nonetheless, strict adherence to daily drug regimens are required to suppress viral replication and restore functional immunity.[1, 2] Yet rigorous adherence is challenging, especially considering the requirement for daily lifelong medication.[3, 4] This requirement may soon be supplanted by long-acting (LA) dosage forms of antiretroviral drugs (ARVs) such as implants and injectable formulations. LA formulations have previously found utility as contraceptives and antipsychotics, and parallel directives are now being considered for HIV-1 prevention and maintenance.[5–7] As of now, HIV-1 LA agents are focused on parenteral cabotegravir (CAB LA) and rilpivirine (RPV LA).[8–10] Specifically, the First LA Injectable Regimen (FLAIR) studied in phase 3 trials and requiring monthly intramuscular (IM) injections was found to be non-inferior to standard oral dolutegravir (DTG), abacavir (ABC), and lamivudine (3TC) at 48 weeks of study.[11] Moreover, the results coincide with the prior Long-Acting Antiretroviral Treatment Enabling Study (LATTE) and current Antiretroviral Therapy as Long Acting Suppression (ATLAS) trials and positive patient feedback for LA ARVs.[11–13] Therefore, anticipating a paradigm shift towards LA ART, innovative formulation designs are required to combat current limitations of large dosage volumes, injection site reactions, suboptimal tissue penetrance and dosing frequency.[14] Alternative to injectable formulations, implantable devices also exhibit consistent and sustained drug release.[15–18] However, the latter approaches require more sophisticated insertion and removal procedures and do not readily facilitate ARV delivery to viral reservoirs. As an alternative our own laboratories LA slow effective release ART (LASER ART) utilizes ARV prodrug modifications to provide slow drug dissolution, penetration of biological membranes, as well as sustained delivery of efficacious drug concentrations to both plasma and tissue reservoirs.[19] LASER ART was developed across a broad spectrum of ARVs and represents an innovative approach towards extending existing LA formulations.[20–22] Therefore, our aim is to synthesize a library of prodrugs for the non-nucleoside reverse transcriptase inhibitor (NNRTI) rilpivirine (RPV), with the objective of developing a novel LA formulation. This is designed to improve tissue drug distribution and prolong the apparent drug half-life of clinically relevant RPV now being developed for human use. To this end, nanoformulation of our lead prodrug candidate M3RPV (NM3RPV), generated RPV plasma concentrations above the PA-IC_{90} (12 ng/mL) for 25 weeks with significant tissue distributions after a single IM injection in *BALB/cJ* mice. Our work provides a proof of concept for a next generation LASER ART for use both as part of a LA regimen and in HIV cure strategies.[23]

2. Materials and Methods

2.1 Reagents

RPV was purchased from LeapChem (Hangzhou, China). Dichloromethane (DCM), tetrahydrofuran (THF), *N,N*-dimethylformamide (DMF), sodium(trimethylsilyl) amide (NaHMDS; 1M in THF), hexanes, ethyl acetate, dimethyl sulfoxide (DMSO), anhydrous pyridine, chloromethyl chlorosulfate, tetrabutylammonium hydrogen sulfate, potassium carbonate, heptanoic acid, lauroyl chloride, myristoyl chloride, stearic acid, zinc chloride ($ZnCl_2$), sodium iodide (NaI), deuterated chloroform, ciprofloxacin, paraformaldehyde (PFA), 3-(4,5-dimethylthiazol-2-yl)-2,5-diphenyltetrazolium bromide (MTT), 3,3'-diaminobenzidine (DAB) and pluronic F127 (P407) were purchased from Sigma-Aldrich (St. Louis, MO). Pluronic F108 (P338) was purchased from BASF (Florham Park, NJ). Acetonitrile (ACN; HPLC and Optima-grade), methanol (MeOH; HPLC and Optima-grade), cell-culture grade water (endotoxin-free), potassium phosphate monobasic (KH_2PO_4), bovine serum albumin (BSA), Triton X-100, and gentamicin were purchased from Fisher Scientific (Hampton, NH). Flash column chromatography was performed on 32–63 μm flash silica gels, while thin layer chromatography utilized pre-coated silica plates (250 μm, F-254) both from SiliCycle Inc. (Quebec, Canada). Dulbecco's Modified Eagle Medium (DMEM) was purchased from Corning Life Sciences (Tewksbury, MA). Polymer-based HRP-conjugated anti-mouse Envision+ secondary antibody and monoclonal mouse anti-human HIV-1 p24 (clone Kal-1) was purchased from Dako (Carpinteria, CA).

2.2 Synthesis of chloromethyl tetradecanoate

Myristoyl chloride was reacted with 1.0 equivalent (eq.) PFA and 0.025 eq. $ZnCl_2$ under reflux conditions for up to 16 hours. The reaction mixture was then cooled to room temperature (RT) and partitioned between DCM and saturated aqueous sodium bicarbonate in a separatory funnel. The aqueous layer was back-extracted twice with DCM. Organic extracts were combined, washed with brine and dried from sodium sulfate. The solvents were evaporated on a rotary evaporator followed by isolation of the desired compound using silica column chromatography eluting with a mobile phase of 9:1 hexanes:ethyl acetate. Chloromethyl-heptanoate, -dodecanoate, and -stearate were synthesized from appropriate fatty acids or acyl chlorides in an analogous manner.

2.3 Synthesis of iodomethyl tetradecanoate

Chloromethyl tetradecanoate (1 eq.) and NaI (2.5 eq.) were dissolved in a 2:1 mixture of ACN/DCM under argon atmosphere. The reaction proceeded for 90 hours at RT under light protection. Upon completion, the mixture was concentrated and partitioned between DCM and water (H_2O). The aqueous layer was further extracted with DCM followed by sequential washing of the combined organic extracts with saturated sodium bicarbonate and brine. The sample solution was then dried from sodium sulfate, concentrated and purified by silica column chromatography eluting with 9:1 hexanes:ethyl acetate. Iodomethyl -heptanoate, -dodecanoate, and -stearate were synthesized from chloromethyl esters using a similar reaction scheme.

2.4 M3RPV synthesis and characterization

RPV hydrochloride (RPV-HCl) was suspended in a mixture (1:1) of anhydrous THF and DMF under an argon atmosphere. The reaction flask was then cooled to −46 °C (ACN-dry ice bath) followed by addition of 3 eq. NaHMDS base and allowed to react for 30 min to deprotonate the secondary amine. A solution of 1.5 eq. iodomethyl tetradecanoate in anhydrous THF was added dropwise followed by gradual warming of the reaction mixture to room temperature and allowed to proceed for 48 hours. The mixture was then cooled to −78 °C, quenched using MeOH and concentrated to remove solvents. The concentrated sample was purified by silica column chromatography eluting with 1:1 hexanes:ethyl acetate to isolate M3RPV with a chemical yield of 53% after precipitation from hexanes. Nuclear magnetic resonance (NMR) and Fourier-transform infrared (FTIR) spectroscopy, as well as positive electrospray ionization mass spectrometry (ESI-MS), were used for characterization. Proton (^{1}H)- and carbon (^{13}C)- NMR spectra were recorded on a Varian Unity/Inova-500 NB (500 MHz; Varian Medical Systems Inc., Palo Alto, CA). FTIR was performed on a PerkinElmer universal attenuated total reflectance (UATR) Spectrum Two (Waltham, MA). ^{1}H NMR (500 MHz, $CDCl_3$): 7.98 (d, J = 5.4 Hz, 1H), 7.79 (d, J = 8.6 Hz, 2H), 7.60 (d, J = 8.3 Hz, 2H), 7.23–7.32 (m, 4H), 5.86–5.95 (m, 2H), 5.51 (d, J = 5.8 Hz, 1H), 2.33 (t, J = 7.2 Hz, 2H), 2.21 (s, 6H), 1.51–1.68 (m, 6H), 1.17–1.32 (m, 17H), 0.87 (t, J = 6.9 Hz, 3H). ^{13}C NMR (125 MHz, $CDCl_3$): δ 173.5, 161.5, 158.9, 157.7, 149.4, 143.9, 141.2, 138.2, 133.8, 133.2, 128.2, 119.4, 118.3, 117.8, 104.4, 97.6, 97.3, 73.0, 34.3, 31.9, 29.6, 29.5, 29.4, 29.3, 29.2, 29.1, 24.8, 22.6, 18.2, 14.1. MS-ES+ (m/z): calcd. for $C_{37}H_{46}N_6O_2$, 606.37 (100%), 607.37 (40.0%), 608.37 (7.8%); found, 607.2 [M+H$^+$]. Synthesis and characterization of M1RPV, M2RPV, and M4RPV was performed in replicate manner (Supplementary Methods, Supplementary Fig. 2–4).

2.5 Quantification of RPV and M3RPV by UPLC-UV/Vis

Drug quantitation was performed on a Waters ACQUITY ultra-performance liquid chromatography (UPLC) H-Class system with TUV detector and Empower 3 software (Milford, MA). RPV and M3RPV samples were separated on a Phenomenex Kinetex 5 μm C18 column (150 × 4.6 mm) (Torrance, CA). RPV was detected at 285 nm, using a mobile phase consisting of 65% 50 mM KH_2PO_4, pH 3.2, and 35% ACN and a flow rate of 1.0 mL/min. M3RPV was detected at 230 nm, using a mobile phase consisting of 90% ACN and 10% H_2O and a flow rate of 1.0 mL/min. Drug content was determined relative to peak areas from drug standards (0.05–50 μg/mL) in MeOH.

2.6 Solubility

Aqueous and 1-octanol solubilities were evaluated by mixing with excess drug (RPV or M3RPV) for 24 hours. Centrifugation at 20,000 *g* for 10 min pelleted any undissolved drug. Aqueous supernatants were frozen, lyophilized, and subsequently resuspended in MeOH for analysis. 1-octanol supernatants were prepared for analysis by dilution into MeOH. Collected samples were analyzed for drug content by UPLC-UV/Vis as described above.

2.7 Nanoparticle manufacture and characterization

Nanoformulations of RPV and M3RPV (NRPV and NM3RPV, respectively) were manufactured using an Avestin EmulsiFlex-C3 high-pressure homogenizer (Ottawa, ON, Canada). NRPV was prepared to best replicate RPV LA developed by Janssen.[24, 25] Specifically, 1% (w/v) P338 was dispersed in H_2O, followed by the addition of 10% (w/v) RPV-free base and mixing overnight. Similarly, NM3RPV contained 2.1% P407 and 21% M3RPV in H_2O. Formulations were homogenized at 20,000 psi to generate homogeneous nanocrystals of uniform size and polydispersity (PDI). Nanoparticle physicochemical characterization for size (nm), PDI and zeta potential (mV) were evaluated by dynamic light scattering (DLS, Malvern Nano-ZS, Worcestershire, UK). NM3RPV and NRPV drug quantitation was analyzed by UPLC-UV/Vis as described above.

2.8 Macrophage cellular uptake and retention studies

Human monocytes were obtained by leukapheresis from HIV-1/2 and hepatitis B seronegative donors and subsequently purified by counter-current centrifugal elutriation.[26] Monocytes were grown in DMEM culture media containing 4.5 g/L glucose, L-glutamine, and sodium pyruvate supplemented with 10% pooled human serum (heat-inactivated), 10 μg/mL ciprofloxacin, and 50 μg/mL gentamicin. Cells were maintained at 37 °C in a 5% CO_2 incubator. Human monocytes were plated in 12, 24, or 96-well plates at 1.0×10^6, 0.5×10^6, or 0.15×10^6 cells/mL respectively. Recombinant human macrophage colony stimulating factor (MCSF, 1000 U/mL) was added to culture media for 7 days to facilitate monocyte-derived macrophages (MDMs) differentiation and vitality in culture. MDM uptake and retention studies were performed in 12-well plates, with each treatment group completed in triplicate. Briefly, MDMs were treated with NM3RPV or NRPV at concentrations of 10 or 30 μM and cells were collected 1, 2, 4 and 8 hours later. For cellular retention studies, drug was removed after 8 hours. Cells were washed with phosphate buffered saline (PBS) and replenished with fresh media. Cellular samples were collected at 1, 5, 10, 20 and 30 days to assay intracellular drug concentration. For both studies, MDMs were collected by removing media, PBS washing 2 times, and scraping the cells into PBS. Cells were subsequently counted using an Invitrogen Countess Automated Cell Counter (Carlsbad, CA). Collected MDMs were centrifuged at 956 *g* for 8 min. Cell pellets were sonicated in MeOH to extract intracellular drug and subsequently centrifuged at 20,000 g for 10 min. Samples were analyzed by UPLC-UV/Vis for intracellular drug content as described above.

2.9 Assay of antiretroviral activities in MDM

For antiretroviral activity assay, MDMs were plated in 24-well plates at a density of 0.5×10^6 cells/well. Cells were treated with 10 or 30 μM NM3RPV or NRPV for 8 hours, followed by a PBS wash and addition of fresh media. Cells were then challenged with HIV-1_{ADA} at a multiplicity of infection (MOI) 0.1 infectious particles per cell at 1, 5, 10, 20 or 30 days after treatment for 16 hours. After viral challenge, cells were washed with PBS and replenished with fresh media. Supernatants were collected 10 days after challenge and assayed for HIV-1 reverse transcriptase (RT) activity.[27, 28] Replicate cells were fixed with 4% PFA and stained for HIV-1p24 antigen by immunohistochemical tests.[28]

2.10 Half-maximum effective concentration (EC_{50}) assays

Studies to determine the EC_{50} of M3RPV and RPV in MDMs were performed in 96-well plates at a density of 0.15×10^6 cells/well. Specifically, cells were treated with 0.1–1000 nM RPV or M3RPV for 2 hours, followed by HIV-1_{ADA} challenge at a MOI of 0.1 for 4 hours. Following viral challenge, cells were washed with PBS, and given fresh (0.1–1000 nM) drug containing media. Subsequently, cell supernatants were collected 10 days later and assayed for HIV-1 RT activity.[27, 28] Replicate studies were performed in CEM-CD4+ T-cell cultures.[29] Specifically, cells were plated in 96-well plates, centrifuged at 650 *g* for 5 min and resuspended in (0.1–1000 nM) drug-containing media for 1 hour. Next, cells were challenged with HIV-$1_{NL4–3\text{-}eGFP}$ at a MOI of 0.1 by spin-inoculation for 2 hours followed by a 16-hour incubation. Subsequently, cells were washed with PBS and fresh (0.1–1000 nM) drug containing media added. Supernatants were collected 10 days after viral challenge to assay HIV-1 RT activity.[27, 28]

2.11 Plasma cleavage kinetics

Plasma cleavage kinetics of M3RPV was evaluated in mouse, rat, rabbit, dog, monkey, and human plasma. M3RPV (1 μM) was incubated in 100 μL plasma at 37 °C. At 0, 2, 6, and 24 hours samples were quenched with 1 mL of MeOH and vortexed for 3 min. Samples were then centrifuged at 15,000 *g* for 10 min; after supernatants were analyzed for M3RPV and/or RPV by UPLC-MS/MS as described below. Heat-inactivated plasma was used as a negative control for enzymatic cleavage and hydrolysis testing.

2.12 Transmission Electron Microscopy (TEM)

Morphology of NRPV and NM3RPV was assessed by TEM using an FEI Tecnai G2 Spirit TEM (Hillsboro, OR) and negative staining. Briefly, 10 μL of diluted nanoformulation was applied to a formavar/silicone monoxide coated 200 mesh copper grid and allowed to absorb for 5 min. Excess sample was removed with filter paper and subsequently dried for an additional 2–5 min. Next, Nanovan negative stain was pipetted onto the grid for staining before imaging under TEM.

2.13 Pharmacokinetics (PK) and biodistribution (BD)

Male *BALB/cJ* mice (6–8 weeks, Jackson Labs, Bar Harbor, ME) were administered 45, 75, or 100 mg/kg RPV-eq. of NM3RPV or NRPV by a single intramuscular (IM; caudal thigh muscle) injection at 40 μL/25 g mouse. Following injection, blood samples were collected into heparinized tubes the following day by cheek puncture, then weekly for the 46 week study duration. Collected blood (25 μL) was immediately diluted into 1 mL ACN and stored at −80 °C until drug analysis. Remaining blood samples were centrifuged at 2,000 *g* for 5 min. Plasma supernatants were collected and stored at −80 °C until further analysis. Animals were humanly euthanized by isoflourane inhalation, followed by cervical dislocation, 56 and 323 days after drug treatment to obtain spleen, lymph node, liver, lung, gut, kidney, brain and rectal tissue for drug content determinations. Drug concentrations in plasma, tissue and whole blood were determined by UPLC-MS/MS using a Waters Acquity UPLC-Xevo TQ-S micro mass spectrometry system (Milford, MA). RPV was separated using an AQUITY UPLC-BEH shield RP18 column (1.7 μm, 2.1 mm × 100 mm) with a 7 min gradient mobile

phase consisting of A (7.5 mM ammonium bicarbonate in Optima-grade H_2O adjusted to pH 7 using acetic acid) and B (100% Optima-grade MeOH) at a flow rate of 0.25 mL/min. Mobile phase B remained at 70% for the initial 4.75 min, followed by an increase to 95% B in 0.25 min and held constant for 0.75 min. Mobile phase B was reset to 70% in 0.25 min and the column equilibrated for 1.0 min before the next injection. A cone voltage of 92 volts and collision energy of 56 volts were used to detect RPV. Multiple reaction monitoring (MRM) transition 367.032 > 127.859 m/z was used for RPV quantification. Internal standards (IS; indinavir (IDV) 250 ng/mL; lopinavir (LPV) 500 ng/mL) was monitored at MRM transition 614.14 > 97.023 and 629.18 > 155.03 m/z respectively. M3RPV was separated using an ACQUITY UPLC-BEH C18 column (1.7 μm, 2.1 mm × 30 mm) with an ACQUITY BEH C18 Vanguard column using a flow rate of 0.28 mL/min. The MRM transition 607.34 > 379.09 m/z was used for MRPV quantification. Mobile phase A consisted of 7.5 mM ammonium formate in Optima-grade H_2O (adjusted to pH 3) and mobile phase B was 100% Optima-grade MeOH. The initial mobile phase composition was 85% B for the first 5 min, then increased to 95% B over 0.25 min, and then held constant for 1.5 min. Mobile phase B was then reset to 85% over 0.25 min and the column was equilibrated for one min before the next injection. For drug analysis 25 μL of plasma was mixed with 1 mL of ice cold ACN and subsequently spiked with 10 μL of IS (MDTG; (630.2 > 420.07) 200 ng/mL IDV; 250 ng/mL LPV; 500 ng/mL). Samples were subsequently vortexed for 3 min and centrifuged at 17,000 *g* for 10 min. Supernatants were dried, reconstituted in 80% MeOH, and 10 μL injected for UPLC-MS/MS analysis. Plasma standards were extracted at a final concentration of 0.1–1000 ng/mL. Tissue analysis required between 20–200 mg of tissue (spleen, lymph node, liver, gut, lung, kidney, brain, rectal) to be diluted with 90% MeOH and homogenized. Tissue homogenates were mixed with MeOH containing IS and vortexed for 3 min, followed by centrifugation at 17,000 *g* for 10 min. Supernatants were collected and mixed with Optima-grade H_2O for UPLC-MS/MS analysis. Tissue standards were extracted at a final concentration of 0.5–2500 ng/mL.

2.14 NM3RPV PK in rhesus macaques

Male rhesus macaques (4.4–6.7 kg; PrimeGen) were anesthetized with ketamine (10 mg/kg) and subsequently administered 45 mg/kg RPV-eq. of NM3RPV and a lab-generated CAB prodrug by IM injection (0.5 mL/kg). Blood samples were collected in potassium-EDTA coated tubes for complete blood counts (CBC), metabolic panels and plasma drug quantitation. Tissue biopsies were performed for lymph node, adipose and rectal tissues at 204 days after injection.

2.15 PK parameter analyses

Non-compartmental PK analysis for plasma RPV was performed using Phoenix WinNonlin-8.0 (Certara, Princeton, NJ, USA) for *BALB/cJ* mice studies.

2.16 Statistics

In vitro studies were expressed as mean ± SEM with a minimum of 3 biological replicates, while in vivo study results were expressed as mean ± SEM with a minimum of 4 biological replicates. GraphPad Prism 7.0 software (La Jolla, CA) was used for all statistical analysis. Specifically, comparisons between two groups utilized Student's *t* test (two-tailed).

Significant differences were denoted as follows: * $P < 0.05$, ** $P < 0.01$, *** $P < 0.001$, **** $P < 0.0001$.

2.17 Study approval

All animal studies were approved by the University of Nebraska Medical Center Institutional Animal Care and Use Committee (IACUC) in accordance with the standards incorporated in the Guide of the Care and Use of Laboratory Animals (National Research Council of the National Academies, 2011). Human monocytes were isolated by leukopheresis from HIV-1/2 and hepatitis B seronegative donors according to an approved UNMC Institutional Review Board exempt protocol.

3. Results

3.1 RPV prodrug synthesis and characterization

RPV was modified by the addition of aliphatic fatty acid chains of differential lengths to develop a diverse library of N-acyloxyalkyl prodrugs (M1RPV, M2RPV, M3RPV, M4RPV; Fig. 1A). FTIR analysis of each prodrug revealed absorption bands between 1726–1734 cm^{-1} corresponding to the carbonyl (C=O) group within the modifying fatty acid (Fig. 1B). Bands between 2852–2864 and 2918–2928 cm^{-1} represent alkane stretches along the aliphatic carbon chain. Nitrile stretches characteristic of the RPV backbone were observed at 2218 cm^{-1}. The ^{1}H NMR spectrum of each prodrug exhibited multiplet signals in the range of 5.57–6.0 and 1.17–1.35 ppm corresponding to the methylene ester and repeating (R-C$\mathbf{H_2}$-R) protons of the attached lipid chain (Fig. 1C). Additionally, chemical shifts between 0.84–0.88 and 2.32–2.33 ppm identified the terminal methyl group (C$\mathbf{H_3}$-R) and C_α protons of the fatty acid chain. The appearance of multiple signals between 22.4 and 34.3 ppm in the ^{13}C NMR spectrum of each prodrug confirmed the carbon atoms of the conjugated aliphatic chain (Supplementary Fig. 1–4). ESI-MS affirmed the molecular weight of all RPV prodrugs (Supplementary Fig. 1–4). Prodrugs were evaluated for physicochemical properties, stability, antiretroviral activity, drug loading capacity and PK and BD. All were used to generate go-no go criteria enabling the generation of a principal drug candidate (Supplementary Fig. 5 and 6). The lead compound, M3RPV, which contains a bioreversible myristic acid, was produced with a chemical yield of 53%. Prodrug synthesis enabled the required alterations of RPV's physicochemical properties. M3RPV exhibited a 2.4-fold decrease in aqueous (** $P < 0.01$) and an 8.7-fold increase in octanol solubility (****P < 0.0001). These data underscored changes in hydrophobicity and lipophilicity generated by the prodrug modifications (Fig. 2A and 2B). Prodrugs are pharmacologically inactive compounds that require enzymatic or hydrolytic activation, thus we tested cleavage kinetics of the M3RPV in mouse, rat, rabbit, dog, monkey and human plasma. Notably, species-specific kinetic differences were observed. Mouse plasma produced the most robust cleavage (94.8%), while human plasma exhibited slower prodrug breakdown (15.7%) over a 24-hour period (Fig. 2C). As successful bioconversion requires removal of the inactive moiety and release of the active compound, we analyzed RPV formation during plasma cleavage. M3RPV incubated in mouse plasma efficiently released 70% of RPV within 24 hours (Fig. 2D). In comparison, dog, human and monkey yielded 5, 14, and 21% RPV, respectively. While different plasma from divergent animal species shows variance in prodrug hydrolysis rates these differences

in metabolism of ester prodrugs is both an important component of preclinical drug development and in assessing pharmacokinetic tests. Prior works, from other laboratories, has shown that the stability and metabolizing enzymes in dog, guinea pig mouse, rat, monkey and human plasma are divergent. [30] That is due in measure to the known divergence in levels and efficiencies of plasma esterases [31]. The cleavage efficiencies of ester bonds reflect different esterase amongst species and are determined through the use of pathway inhibitors involved in the hydrolysis reactions. [32]

To demonstrate there was not an abrogation of activity due to prodrug modification, M3RPV was tested against HIV-1 in both MDM and CEM-CD4+ T-cells. M3RPV exhibited a 4.3-fold increase in EC_{50} compared with RPV (8.2 nM vs 1.9 nM respectively). In the CEM T-cell line, M3RPV demonstrated a 6.8-fold increase in EC_{50} compared with RPV (5.5 nM vs 0.8 nM respectively).

3.2. Nanoformulation characterization and particle stability

NRPV and NM3RPV were manufactured by top down synthesis utilizing high-pressure homogenization to generate stable nanosuspensions. Poloxamer (P338 and P407) surfactants provided particle surface stabilization for NRPV and NM3RPV, respectively. As clinically relevant injectable formulations must maintain their physical integrity within a range of storage conditions, DLS was used to assess physicochemical stability of NRPV and NM3RPV at room temperature (RT), 4 °C, and 37 °C. Both formulations maintained particle size, PDI, and zeta potential for a period of 100 days. Specifically, the initial size (277 ± 9 nm), PDI (0.24 ± 0.02), and zeta potential (−9.2 ± 0.3 mV) of NRPV were stable over the course of testing (239 ± 3 nm, 0.25 ± 0.01, −13.6 ±. 0.7 mV at day 100; Fig. 3A). Of note, while the zeta potential is used as quantification of particle-drug charge magnitude is may not indicate structure or electric surface potential. TNM3RPV had an average particle size of 345 ± 5 nm, PDI of 0.18 ± 0.06 and zeta potential of −17.6 ± 0.6 mV at the time of manufacture. One hundred days later, physicochemical parameters of NM3RPV were stable (326 ± 1 nm, 0.25 ± 0.1 and −9.2 ± 0.9 mV; Fig. 3D). Furthermore, temperature variation (4° or 37 °C) did not change the physical integrity of either NRPV or NM3RPV (Fig. 3B,C,E,F) Transmission electron microscopy (TEM) of both NRPV and NM3RPV displayed nanocrystals of an elongated cuboidal morphology (Fig 3G,H). Importantly, we determined prodrug stability within NM3RPV over time. NM3RPV contained 99.7% M3RPV when analyzed for both prodrug and parent RPV compounds by UPLC-UV/Vis after initial manufacture. By day 100 the percentage remained consistent for NM3RPV at RT and 4 °C (99.7%), while a decreasing trend was observed in formulation stored at 37 °C (99.4%) (Fig. 3I). Furthermore, PK tests of NM3RPV in *BALB/cJ* mice comparing freshly made formulations to those stored at RT for 90 days showed that plasma RPV levels were comparable between the formulations during the 147-day testing period (Supplementary Fig. 7).

3.3 NM3RPV-macrophage interactions

The phagocytic nature of macrophages affords testing of their use as cellular drug depots. We therefore evaluated uptake of NM3RPV and NRPV in MDM at 10 and 30 μM concentrations. Drug formulations administered at 10 μM resulted in comparable

intracellular drug levels after 8 hours for NM3RPV (2.0 μg/10^6 cells) and NRPV (2.2 μg/10^6 cells) (Fig. 4A). A 30 μM treatment led to drug concentrations of 6.0 μg/10^6 cells and 4.9 μg/10^6 cells for NRPV and NM3RPV, respectively (Fig. 4E). Cellular uptake of NRPV or NM3RPV at either concentration did not induce changes in cellular vitality as measured by MTT assay (Supplementary Fig. 8). Furthermore, NM3RPV treated cells generated detectable intracellular RPV concentrations of 95 and 140 ng/10^6 cells 8 hours after 10 and 30 μM drug exposure, respectively. As macrophages also have the capacity to migrate throughout the body, thereby serving as drug delivery systems to viral reservoirs, we tested their capacity to retain intracellular drug over a 30-day period following a single drug loading. A single exposure of MDM to 10 or 30 μM NM3RPV showed enhanced intracellular drug retention over NRPV. Specifically, the amount of prodrug retained by MDM was 1.7 and 2.9 μg/10^6 cells 30 days after treatment with 10 and 30 μM NM3RPV, respectively (Fig. 4B,F). Conversely, NRPV treatment yielded RPV levels that fell below the limit of quantitation within 20 days, with significantly lower drug concentrations at all time points when compared to NM3RPV treatment. Importantly, at both concentrations (10 and 30 μM) sustained RPV concentrations were detected for 30 days in NM3RPV-treated cells. To examine whether sustained drug retention would protect MDM against HIV-1 infection, we challenged cells with HIV-1_{ADA} up to 30 days following an 8-hour drug loading and assayed quantitatively for HIV-1 RT activity, as well as qualitatively for HIV-1 p24 antigen expression (Fig 4C–D,G–H). Both 10 and 30 μM NM3RPV suppressed HIV-1 RT activity by > 96% at all time points. In contrast, treatment of MDM with 10 μM NRPV provided 67% reduction of HIV-1 RT activity when challenged 10 days post treatment, with complete viral breakthrough occurring at day 20. Similarly, 30 μM NRPV provided a minimal viral inhibition of 42% at day 30. Therefore, enhanced MDM drug retention exhibited by NM3RPV provides superior protection against HIV-1 challenge compared to NRPV.

3.4 PK and BD

Prodrug modification not only alters the physicochemical properties of a compound, but can also change its PK profile and tissue distribution. To assess changes in PK, we administered a single IM injection of 45, 75, or 100 mg/kg RPV-eq. doses of NM3RPV or NRPV to male *BALB/cJ* mice. Neither NRPV nor NM3RPV had any adverse effects on animal weight or presented with any tissue histopathology over the course of study. (Supplementary Fig. 9). NM3RPV generated lower initial plasma RPV concentrations coupled with slower decay kinetics compared to NRPV. Animals dosed with 45, 75, or 100 mg/kg NRPV maintained RPV plasma concentrations above the protein-adjusted 90% inhibitory concentration (PA-IC_{90}; 12 ng/mL) for 4, 6, and 7 weeks, respectively, before falling below the limit of quantitation of 0.5 ng/mL by 10, 13, and 16 weeks, respectively (Fig. 5A). In comparison, NM3RPV demonstrated sustained plasma RPV concentrations above the PA-IC_{90} for 4, 12, and 25 weeks at doses of 45, 75, and 100 mg/kg RPV-eq., respectively. Furthermore, NM3RPV-treated animals exhibited 13- and 26-fold increases in plasma RPV apparent half-life ($t_{1/2}$) and mean residence time (MRT) compared to NRPV, respectively (Supplementary Table 1). NM3RPV significantly improved tissue biodistribution compared to NRPV. Particularly, NM3RPV exhibited significantly higher RPV concentrations in the spleen, liver, gut, and kidney 8 weeks following drug administration across all doses (Fig 5B–F). At the conclusion of study (46 weeks), RPV concentrations were still detectable in most tissues

tested (spleen, lymph node, liver, gut, kidney) from NM3RPV treated animals, with high concentrations observed in the lymph nodes (145 ng/g). By comparison, RPV was not found in any tissue collected 46 weeks after treatment with NRPV. We also assayed all tissues for the presence of M3RPV. Lymph nodes, spleen, and liver were substantial depots for M3RPV, containing 26,941, 674, and 220 ng/g of M3RPV 46 weeks after injection, respectively (Fig. 5B–D). To determine whether differences in M3RPV cleavage kinetics could generate PK differences, NM3RPV was evaluated after a single IM injection of 45 mg/kg RPV-eq. in rhesus macaques. We observed a significant presence of prodrug in plasma, whereby concentrations of M3RPV were between 2- to 16-fold higher than RPV across the course of 44 weeks of investigation (Fig. 6A). Rectal, lymph node, and adipose tissue biopsies collected 204 days after NM3RPV treatment contained measurable levels of both M3RPV and RPV. Specifically, RPV concentrations of 8.7, 23.7, and 19.7 ng/g were detected in the rectal, lymph node and adipose tissues at day 204 (Fig. 6B). M3RPV was present at high levels in lymph node and adipose tissues (456.3 and 532.3 ng/g, respectively), with lower levels detected in rectal tissue (7.4 ng/g; Fig. 6C).

4. Discussion

Treatment of HIV-1 infection requires life-long ART to maintain viral suppression, CD4+ T cell numbers and a normal lifespan.[1, 2] Since inception, ART has required strict adherence for both treatment of existing infection and for pre-exposure prophylaxis.[33] While ART has evolved to forms requiring only a single daily pill,[34] LA formulations, such as injectables or implants, have received considerable patient interest.[35, 36] Sub-Saharan Africa, which bears the largest global burden of HIV-1 infections, has seen increased use of injections or implants for contraception which lays the groundwork for widespread acceptance and use of LA ART in these resource limited settings.[37, 38]

Monthly administrations of CAB LA and RPV LA have demonstrated levels of viral suppression consistent with established oral treatments.[11–13] Therefore, as LA ART comes closer to approval, optimization of delivery and incorporation of a broader range of ARVs are in increasing demand. In parallel, reducing injection volume, dose frequency, and injection site reactions while increasing tissue drug penetrance are key goals of LA ART.[14] While implantable devices can alleviate some of these concerns, cost and access remain limitations.[15–18] In an effort to improve drug biodistribution to viral reservoirs and promote global use, LASER ART was created. It employs a prodrug approach to incorporate ARVs into nanocrystals generating sustained plasma drug concentrations with efficient tissue and cell reservoir delivery.[19–22]

Herein, a novel library of prodrugs were synthesized for RPV. Our present studies focused on the synthesis, nanoformulation, and characterization of a myristoylated RPV (M3RPV). Prodrug modification can change the structure of a compound to achieve a specific goal, such as alteration of physicochemical or PK properties.[36] RPV is a poorly soluble diarylpyrimidine (DAPY) derivative extensively studied as a LA formulation (RPV LA).[24, 25, 39] Previous research has demonstrated that synthesizing hydrophobic prodrugs of inherently low solubility compounds can be beneficial, particularly by increasing the plasma drug apparent half-life and/or enhancing tissue distribution.[20, 21, 40, 41] M3RPV was

manufactured as a LA nanoparticle, coined as NM3RPV, using high-pressure homogenization. For comparison, we best replicated RPV LA, with the manufacture of NRPV. In particular, we used the same surfactant (P338) generating particles of 277 nm, similar to the 200 nm RPV LA formulations.[24, 25] Both preparations use top-down approaches for manufacture.[24, 25]

Stability is important for clinical translation. NM3RPV demonstrated exceptional physicochemical stability at 4 °C and 37 °C over a period of 100 days. Importantly for clinical use, injectable formulations must provide repeatable PK results months after initial manufacture. In our studies, NM3RPV provided congruent RPV concentrations in mouse plasma after injection with both newly prepared and 90 days post manufacture formulations.

Drug delivery to viral reservoirs remains a challenge.[42, 43] LA injectable formulations are designed to generate slow dissolution depots at the injection site. Furthermore, infiltrating macrophages have been observed sequestering nanocrystals at the injection site facilitating their biodistribution.[21, 44] These cells are phagocytic and highly mobile.[45] In particular, macrophages have large cytoplasmic volumes, such that phagocytized drug nanocrystals can be stored for extended time periods.[19, 20, 46] Therefore, nanocrystals can develop a cell-based tissue depot, but also more efficiently deliver drug to sites of viral infection. Prodrug modifications, particularly those that increase lipophilicity, have been observed to increase macrophage drug uptake and retention.[20–22, 47] In our work, NM3RPV and NRPV both readily enter macrophages, but only NM3RPV is retained for a significant period of time, providing evidence NM3RPV may establish a secondary tissue or cellular depot.

Prodrug modification not only significantly alters a compound's physicochemical properties, but also its PK and BD.[48] In our studies, NM3RPV generated substantial differences in the duration of RPV plasma concentrations, as well as tissue distribution, when compared to NRPV. We administered mice 100 mg/kg RPV-eq. in accordance with the human equivalent dose administered in clinical trials, based upon a species scaling factor of 12.3.[11, 12, 49] Prodrug modification provided a shallow plasma decay curve, thereby providing sustained RPV concentrations 46 weeks after injection. Specifically, RPV concentrations were above the proposed PA-IC_{90} (12 ng/mL) for 25 weeks after administration. These results are significant when compared NRPV, which only stayed above the PA-IC_{90} for 7 weeks. Clinical trials demonstrating viral suppression with RPV LA and CAB LA injections every 8 weeks observed RPV C_{trough} concentrations of 64 ng/mL, or ~5 times the PA-IC_{90}.[12] In addition, viral breakthrough was observed in a patient after accidental HIV-1 exposure 41 days after RPV LA injection (300 mg) exhibiting approximately 10.5 ng/mL RPV in plasma on the day of exposure.[50] Therefore, future work must focus on increasing RPV plasma concentrations by optimizing dosing schedules or altering prodrug structure.

To determine whether known species differences in plasma carboxylesterase may affect the in vivo behavior of NM3RPV, rhesus monkeys were given 45 mg/kg RPV-eq. of NM3RPV by IM injection. Treatment resulted in sustained levels of M3RPV in the plasma over the course of 44 weeks, but provided low levels of active RPV, which quickly fell below the PA-IC_{90}. This was in contrast to our observations in mice, which exhibited sustained plasma concentrations of active RPV over 46 weeks. These data paralleled our plasma in vitro

cleavage studies where stark differences in prodrug bioconversion were observed between species (mouse; rhesus macaque), indicating slower conversion of M3RPV to RPV in monkeys. Observed differences in cleavage kinetics may be due to lack of abundant carboxylesterases observed in monkey, dog, and/or human plasma compared to rodents.[51, 52] Certainly multiple plasma esterases likely play a role in the species differences. Future will work will discern the optimal rates of bioactivation and the most effective implementation of prodrug strategies designed to extend the apparent half-lives of antiretroviral drugs. Impending research directives will investigate formulations of shorter chain RPV prodrugs (M1RPV, M2RPV) in rhesus macaques that may provide more rapid bioconversion to active drug.

LASER ART employs hydrophobic and lipophilic prodrugs to enrich tissue distribution, particularly to sites of viral infection. In our mouse studies, NM3RPV generated significant tissue depots in the lymph nodes, spleen, and liver, whereby substantial prodrug concentrations were observed 46 weeks after injection (26941, 674, 220 ng/g, respectively). We posit the considerable prodrug tissue depot, coupled with the slow cleavage kinetics of M3RPV provided sustained RPV concentrations not only in the plasma but in tissue, as RPV was still detectable in spleen, lymph node, liver, gut, and kidney 46 weeks after treatment. These findings provide significant improvements in the long-term distributions of RPV to tissues important in viral replication. Importantly, rhesus macaques also retained substantial concentrations of both M3RPV and RPV in the lymph nodes 204 days after injection.

In conclusion, LA ART is a significant step forward in the field of HIV-1 therapeutics. In particular, RPV LA has garnered excitement with its success coupled with CAB LA in phase 3 clinical trials. In our studies, we generated a LASER ART formulation of RPV by synthesizing a series of hydrophobic prodrugs in an attempt to increase RPV tissue distribution and apparent half-life. Our studies provide an excellent proof-of-concept that nanoformulated prodrugs of RPV can provide sustained release of RPV and generate a significant secondary tissue depot. Further work studying prodrug bioconversion, PK, pharmacodynamics, and injection schedules are required.

Supplementary Material

Refer to Web version on PubMed Central for supplementary material.

Acknowledgements

We wish to thank the University of Nebraska Medicine cores for NMR Spectroscopy (Ed Ezell), Elutriation and Cell Separation (Myhanh Che and Na Ly), Electron Microscopy (Tom Bargar and Nicholas Conoan), as well as Comparative Medicine for technical assistance. Furthermore, we would like to acknowledge Dr. Won-Bin Young and Kamel Khalili at Temple University for HIV-$1_{NL4\text{-}3\text{-}eGFP}$ molecular clone plasmid. The following reagent was obtained through the NIH AIDS Reagent Program, Division of AIDS, NIAID, NIH: CEM CD4+ Cells from Dr. J.P. Jacobs. Thank you to Dr. Samuel Cohen for his tissue toxicological assessments. This research is supported by the University of Nebraska Foundation, which includes donations from the Carol Swarts, M.D. Emerging Neuroscience Research Laboratory, the Margaret R. Larson Professorship, and the Frances and Louie Blumkin, and Harriet Singer Endowments, the Vice Chancellor’s Office of the University of Nebraska Medical Center for Core Facilities and the National Institutes of Health grants P01 DA028555, R01 NS36126, P01 NS31492, 2R01 NS034239, P01 MH64570, P01 NS43985, P30 MH062261 and R01 AG043540, 1 R56 Al138613-01A1.

References

[1]. May MT, Gompels M, Delpech V, Porter K, Orkin C, Kegg S, Hay P, Johnson M, Palfreeman A, Gilson R, Chadwick D, Martin F, Hill T, Walsh J, Post F, Fisher M, Ainsworth J, Jose S, Leen C, Nelson M, Anderson J, Sabin C, Study UKCHC, Impact on life expectancy of HIV-1 positive individuals of CD4+ cell count and viral load response to antiretroviral therapy, Aids, 28 (2014) 1193–1202. [PubMed: 24556869]

[2]. C. Antiretroviral Therapy Cohort, Survival of HIV-positive patients starting antiretroviral therapy between 1996 and 2013: a collaborative analysis of cohort studies, The lancet. HIV, 4 (2017) e349–e356. [PubMed: 28501495]

[3]. Shubber Z, Mills EJ, Nachega JB, Vreeman R, Freitas M, Bock P, Nsanzimana S, Penazzato M, Appolo T, Doherty M, Ford N, Patient-Reported Barriers to Adherence to Antiretroviral Therapy: A Systematic Review and Meta-Analysis, PLoS medicine, 13 (2016) e1002183. [PubMed: 27898679]

[4]. Osterberg L, Blaschke T, Adherence to medication, The New England journal of medicine, 353 (2005) 487–497. [PubMed: 16079372]

[5]. Winner B, Peipert JF, Zhao Q, Buckel C, Madden T, Allsworth JE, Secura GM, Effectiveness of long-acting reversible contraception, The New England journal of medicine, 366 (2012) 1998–2007. [PubMed: 22621627]

[6]. Adams CE, Fenton MK, Quraishi S, David AS, Systematic meta-review of depot antipsychotic drugs for people with schizophrenia, The British journal of psychiatry : the journal of mental science, 179 (2001) 290–299. [PubMed: 11581108]

[7]. Gulick RM, Flexner C, Long-Acting HIV Drugs for Treatment and Prevention, Annual review of medicine, 70 (2019) 137–150.

[8]. Spreen W, Ford SL, Chen S, Wilfret D, Margolis D, Gould E, Piscitelli S, GSK1265744 pharmacokinetics in plasma and tissue after single-dose long-acting injectable administration in healthy subjects, Journal of acquired immune deficiency syndromes, 67 (2014) 481–486. [PubMed: 25140909]

[9]. van ‘t Klooster G, Hoeben E, Borghys H, Looszova A, Bouche MP, van Velsen F, Baert L, Pharmacokinetics and disposition of rilpivirine (TMC278) nanosuspension as a long-acting injectable antiretroviral formulation, Antimicrobial agents and chemotherapy, 54 (2010) 2042–2050. [PubMed: 20160045]

[10]. Spreen WR, Margolis DA, Pottage JC Jr., Long-acting injectable antiretrovirals for HIV treatment and prevention, Current opinion in HIV and AIDS, 8 (2013) 565–571. [PubMed: 24100877]

[11]. Taylor BS, Tieu HV, Jones J, Wilkin TJ, CROI 2019: advances in antiretroviral therapy, Topics in antiviral medicine, 27 (2019) 50–68. [PubMed: 31137003]

[12]. Margolis DA, Gonzalez-Garcia J, Stellbrink HJ, Eron JJ, Yazdanpanah Y, Podzamczer D, Lutz T, Angel JB, Richmond GJ, Clotet B, Gutierrez F, Sloan L, Clair MS, Murray M, Ford SL, Mrus J, Patel P, Crauwels H, Griffith SK, Sutton KC, Dorey D, Smith KY, Williams PE, Spreen WR, Long-acting intramuscular cabotegravir and rilpivirine in adults with HIV-1 infection (LATTE-2): 96-week results of a randomised, open-label, phase 2b, non-inferiority trial, Lancet, 390 (2017) 1499–1510. [PubMed: 28750935]

[13]. Kerrigan D, Mantsios A, Gorgolas M, Montes ML, Pulido F, Brinson C, deVente J, Richmond GJ, Beckham SW, Hammond P, Margolis D, Murray M, Experiences with long acting injectable ART: A qualitative study among PLHIV participating in a Phase II study of cabotegravir + rilpivirine (LATTE-2) in the United States and Spain, PloS one, 13 (2018) e0190487. [PubMed: 29304154]

[14]. Gendelman HE, McMillan J, Bade AN, Edagwa B, Kevadiya BD, The Promise of Long-Acting Antiretroviral Therapies: From Need to Manufacture, Trends in microbiology, 27 (2019) 593–606. [PubMed: 30981593]

[15]. Kovarova M, Benhabbour SR, Massud I, Spagnuolo RA, Skinner B, Baker CE, Sykes C, Mollan KR, Kashuba ADM, Garcia-Lerma JG, Mumper RJ, Garcia JV, Ultra-long-acting removable drug delivery system for HIV treatment and prevention, Nature communications, 9 (2018) 4156.

[16]. Gunawardana M, Remedios-Chan M, Miller CS, Fanter R, Yang F, Marzinke MA, Hendrix CW, Beliveau M, Moss JA, Smith TJ, Baum MM, Pharmacokinetics of long-acting tenofovir alafenamide (GS-7340) subdermal implant for HIV prophylaxis, Antimicrobial agents and chemotherapy, 59 (2015) 3913–3919. [PubMed: 25896688]

[17]. Flexner C, Antiretroviral implants for treatment and prevention of HIV infection, Current opinion in HIV and AIDS, 13 (2018) 374–380. [PubMed: 29794816]

[18]. Barrett SE, Teller RS, Forster SP, Li L, Mackey MA, Skomski D, Yang Z, Fillgrove KL, Doto GJ, Wood SL, Lebron J, Grobler JA, Sanchez RI, Liu Z, Lu B, Niu T, Sun L, Gindy ME, Extended-Duration MK-8591-Eluting Implant as a Candidate for HIV Treatment and Prevention, Antimicrobial agents and chemotherapy, 62 (2018).

[19]. Edagwa B, McMillan J, Sillman B, Gendelman HE, Long-acting slow effective release antiretroviral therapy, Expert opinion on drug delivery, 14 (2017) 1281–1291. [PubMed: 28128004]

[20]. Sillman B, Bade AN, Dash PK, Bhargavan B, Kocher T, Mathews S, Su H, Kanmogne GD, Poluektova LY, Gorantla S, McMillan J, Gautam N, Alnouti Y, Edagwa B, Gendelman HE, Creation of a long-acting nanoformulated dolutegravir, Nature communications, 9 (2018) 443.

[21]. Zhou T, Su H, Dash P, Lin Z, Dyavar Shetty BL, Kocher T, Szlachetka A, Lamberty B, Fox HS, Poluektova L, Gorantla S, McMillan J, Gautam N, Mosley RL, Alnouti Y, Edagwa B, Gendelman HE, Creation of a nanoformulated cabotegravir prodrug with improved antiretroviral profiles, Biomaterials, 151 (2018) 53–65. [PubMed: 29059541]

[22]. Lin Z, Gautam N, Alnouti Y, McMillan J, Bade AN, Gendelman HE, Edagwa B, ProTide generated long-acting abacavir nanoformulations, Chemical communications, 54 (2018) 8371–8374. [PubMed: 29995046]

[23]. Dash PK, Kaminski R, Bella R, Su H, Mathews S, Ahooyi TM, Chen C, Mancuso P, Sariyer R, Ferrante P, Donadoni M, Robinson JA, Sillman B, Lin Z, Hilaire JR, Banoub M, Elango M, Gautam N, Mosley RL, Poluektova LY, McMillan J, Bade AN, Gorantla S, Sariyer IK, Burdo TH, Young WB, Amini S, Gordon J, Jacobson JM, Edagwa B, Khalili K, Gendelman HE, Sequential LASER ART and CRISPR Treatments Eliminate HIV-1 in a Subset of Infected Humanized Mice, Nature communications, 10 (2019) 2753.

[24]. Williams PE, Crauwels HM, Basstanie ED, Formulation and pharmacology of long-acting rilpivirine, Current opinion in HIV and AIDS, 10 (2015) 233–238. [PubMed: 26049947]

[25]. Baert L, van ‘t Klooster G, Dries W, Francois M, Wouters A, Basstanie E, Iterbeke K, Stappers F, Stevens P, Schueller L, Van Remoortere P, Kraus G, Wigerinck P, Rosier J, Development of a long-acting injectable formulation with nanoparticles of rilpivirine (TMC278) for HIV treatment, European journal of pharmaceutics and biopharmaceutics : official journal of Arbeitsgemeinschaft fur Pharmazeutische Verfahrenstechnik e.V, 72 (2009) 502–508. [PubMed: 19328850]

[26]. Gendelman HE, Orenstein JM, Martin MA, Ferrua C, Mitra R, Phipps T, Wahl LA, Lane HC, Fauci AS, Burke DS, et al., Efficient isolation and propagation of human immunodeficiency virus on recombinant colony-stimulating factor 1-treated monocytes, The Journal of experimental medicine, 167 (1988) 1428–1441. [PubMed: 3258626]

[27]. Kalter DC, Greenhouse JJ, Orenstein JM, Schnittman SM, Gendelman HE, Meltzer MS, Epidermal Langerhans cells are not principal reservoirs of virus in HIV disease, Journal of immunology, 146 (1991) 3396–3404.

[28]. Nowacek AS, McMillan J, Miller R, Anderson A, Rabinow B, Gendelman HE, Nanoformulated antiretroviral drug combinations extend drug release and antiretroviral responses in HIV-1-infected macrophages: implications for neuroAIDS therapeutics, Journal of neuroimmune pharmacology : the official journal of the Society on NeuroImmune Pharmacology, 5 (2010) 592–601. [PubMed: 20237859]

[29]. Foley GE, Lazarus H, Farber S, Uzman BG, Boone BA, McCarthy RE, Continuous Culture of Human Lymphoblasts from Peripheral Blood of a Child with Acute Leukemia, Cancer, 18 (1965) 522–529. [PubMed: 14278051]

[30]. Bahar FG, Ohura K, Ogihara T, Imai T Species difference of esterase expression and hydrolase activity in plasma, Journal of Pharmaceutical Sciences, 101 (2012) 3939–3988.

[31]. Berry LM, Wollenberg L, Zhao Z Esterase activities in the blood, liver and intesting of several preclinial species and humans Drug Metabolism Letters 3 (2009) 70–77.

[32]. Lavis LD Ester bonds in prodrugs. ACS Chem. Biol. 4 (2008) 203–206.

[33]. Haberer JE, Current concepts for PrEP adherence in the PrEP revolution: from clinical trials to routine practice, Current opinion in HIV and AIDS, 11 (2016) 10–17. [PubMed: 26633638]

[34]. Gandhi M, Gandhi RT, Single-pill combination regimens for treatment of HIV-1 infection, The New England journal of medicine, 371 (2014) 248–259. [PubMed: 25014689]

[35]. Williams J, Sayles HR, Meza JL, Sayre P, Sandkovsky U, Gendelman HE, Flexner C, Swindells S, Long-acting parenteral nanoformulated antiretroviral therapy: interest and attitudes of HIV-infected patients, Nanomedicine, 8 (2013) 1807–1813. [PubMed: 23611617]

[36]. Murray MI, Markowitz M, Frank I, Grant RM, Mayer KH, Hudson KJ, Stancil BS, Ford SL, Patel P, Rinehart AR, Spreen WR, Margolis DA, Satisfaction and acceptability of cabotegravir long-acting injectable suspension for prevention of HIV: Patient perspectives from the ECLAIR trial, HIV clinical trials, 19 (2018) 129–138. [PubMed: 30445896]

[37]. Kharsany AB, Karim QA, HIV Infection and AIDS in Sub-Saharan Africa: Current Status, Challenges and Opportunities, The open AIDS journal, 10 (2016) 34–48. [PubMed: 27347270]

[38]. Rattan J, Noznesky E, Curry DW, Galavotti C, Hwang S, Rodriguez M, Rapid Contraceptive Uptake and Changing Method Mix With High Use of Long-Acting Reversible Contraceptives in Crisis-Affected Populations in Chad and the Democratic Republic of the Congo, Global health, science and practice, 4 Suppl 2 (2016) S5–S20.

[39]. Rautio J, Kumpulainen H, Heimbach T, Oliyai R, Oh D, Jarvinen T, Savolainen J, Prodrugs: design and clinical applications, Nature reviews. Drug discovery, 7 (2008) 255–270. [PubMed: 18219308]

[40]. Verloes R, Deleu S, Niemeijer N, Crauwels H, Meyvisch P, Williams P, Safety, tolerability and pharmacokinetics of rilpivirine following administration of a long-acting formulation in healthy volunteers, HIV medicine, 16 (2015) 477–484. [PubMed: 25988676]

[41]. Turncliff R, Hard M, Du Y, Risinger R, Ehrich EW, Relative bioavailability and safety of aripiprazole lauroxil, a novel once-monthly, long-acting injectable atypical antipsychotic, following deltoid and gluteal administration in adult subjects with schizophrenia, Schizophrenia research, 159 (2014) 404–410. [PubMed: 25266547]

[42]. Bishara D, Once-monthly paliperidone injection for the treatment of schizophrenia, Neuropsychiatric disease and treatment, 6 (2010) 561–572. [PubMed: 20856919]

[43]. Lorenzo-Redondo R, Fryer HR, Bedford T, Kim EY, Archer J, Pond SLK, Chung YS, Penugonda S, Chipman J, Fletcher CV, Schacker TW, Malim MH, Rambaut A, Haase AT, McLean AR, Wolinsky SM, Persistent HIV-1 replication maintains the tissue reservoir during therapy, Nature, 530 (2016) 51–56. [PubMed: 26814962]

[44]. Darville N, van Heerden M, Vynckier A, De Meulder M, Sterkens P, Annaert P, Van den Mooter G, Intramuscular administration of paliperidone palmitate extended-release injectable microsuspension induces a subclinical inflammatory reaction modulating the pharmacokinetics in rats, Journal of pharmaceutical sciences, 103 (2014) 2072–2087. [PubMed: 24845884]

[45]. Aderem A, Underhill DM, Mechanisms of phagocytosis in macrophages, Annual review of immunology, 17 (1999) 593–623.

[46]. Nowacek AS, Miller RL, McMillan J, Kanmogne G, Kanmogne M, Mosley RL, Ma Z, Graham S, Chaubal M, Werling J, Rabinow B, Dou H, Gendelman HE, NanoART synthesis, characterization, uptake, release and toxicology for human monocyte-macrophage drug delivery, Nanomedicine, 4 (2009) 903–917. [PubMed: 19958227]

[47]. Singh D, McMillan J, Hilaire J, Gautam N, Palandri D, Alnouti Y, Gendelman HE, Edagwa B, Development and characterization of a long-acting nanoformulated abacavir prodrug, Nanomedicine, 11 (2016) 1913–1927. [PubMed: 27456759]

[48]. Huttunen KM, Raunio H, Rautio J, Prodrugs--from serendipity to rational design, Pharmacological reviews, 63 (2011) 750–771. [PubMed: 21737530]

[49]. Nair AB, Jacob S, A simple practice guide for dose conversion between animals and human, Journal of basic and clinical pharmacy, 7 (2016) 27–31. [PubMed: 27057123]

[50]. Penrose KJ, Parikh UM, Hamanishi KA, Else L, Back D, Boffito M, Jackson A, Mellors JW, Selection of Rilpivirine-Resistant HIV-1 in a Seroconverter From the SSAT 040 Trial Who Received the 300-mg Dose of Long-Acting Rilpivirine (TMC278LA), The Journal of infectious diseases, 213 (2016) 1013–1017. [PubMed: 26563240]

[51]. Bahar FG, Ohura K, Ogihara T, Imai T, Species difference of esterase expression and hydrolase activity in plasma, Journal of pharmaceutical sciences, 101 (2012) 3979–3988. [PubMed: 22833171]

[52]. Wang D, Zou L, Jin Q, Hou J, Ge G, Yang L, Human carboxylesterases: a comprehensive review, Acta pharmaceutica Sinica. B, 8 (2018) 699–712. [PubMed: 30245959]

[53]. Wong JK, Yukl SA, Tissue reservoirs of HIV, Current opinion in HIV and AIDS, 11 (2016) 362–370. [PubMed: 27259045]

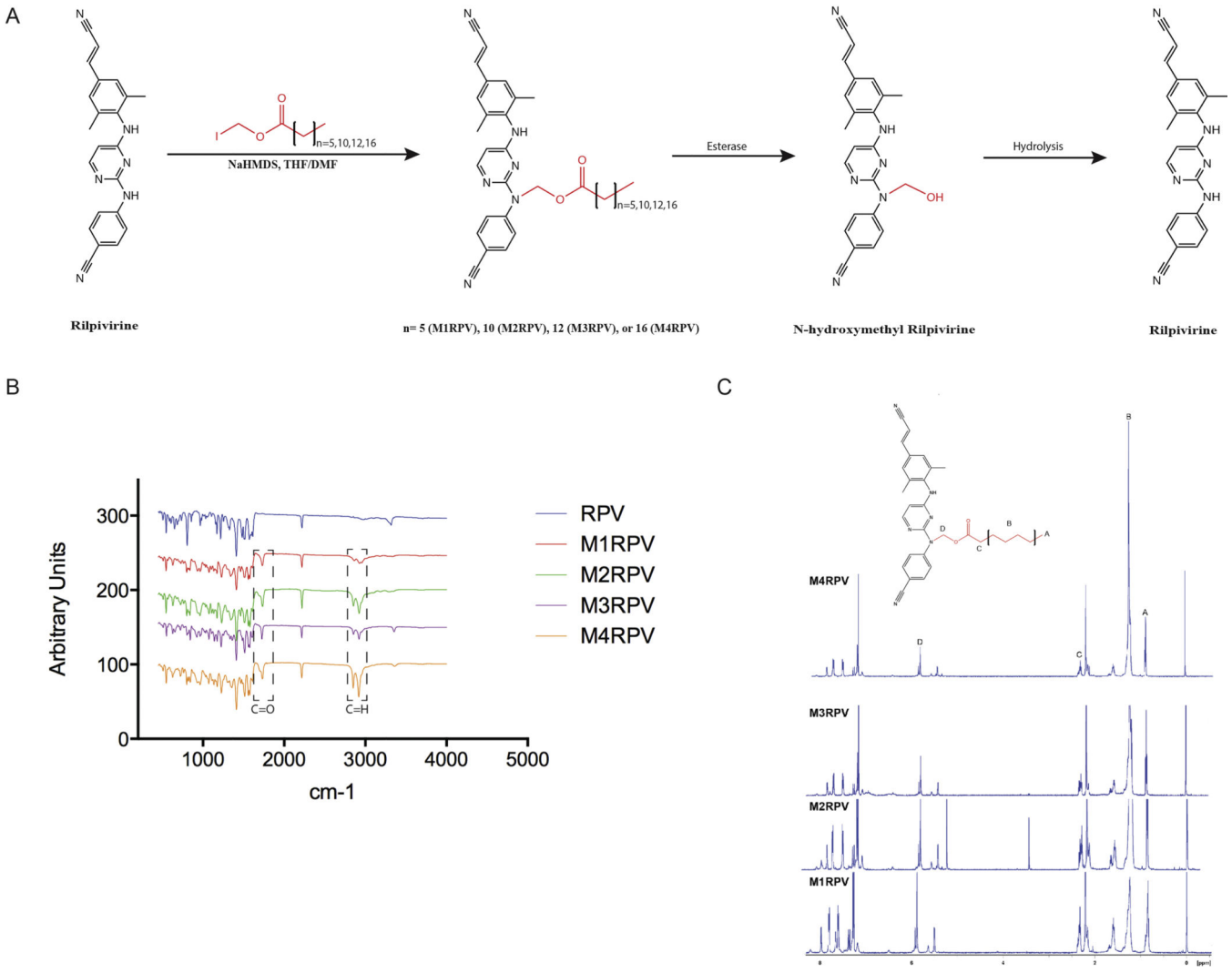

Figure 1. Synthesis of RPV prodrugs.

(A) RPV was modified with variable fatty acid chain lengths (7, 12, 14 and 18 carbon) to develop a library of prodrugs (M1RPV, M2RPV, M3RPV, and M4RPV, respectively). Prodrug bioconversion is hypothesized to first proceed by enzymatic cleavage of the methylene ester, yielding N-hydroxymethyl RPV. Subsequently, hydrolysis will yield the original active compound (RPV). **(B)** FTIR spectroscopy produced absorption bands between 1726–1730 cm^{-1}, as well as (2852–2864 and 2918–2928 cm^{-1}), representing aliphatic chain carbonyl and alkane stretches, respectively. **(C)** Proton NMR spectra confirmed the synthesis of each RPV prodrug. Specifically, multiplet signals between 5.57–6.0 ppm and 1.17–1.35 ppm correspond to the methylene ester and repeating (R-C**H_2**-R) protons respectively. In addition, C_α and terminal methyl group protons are identified between 2.32–2.33 ppm and 0.84–0.87 ppm, respectively.

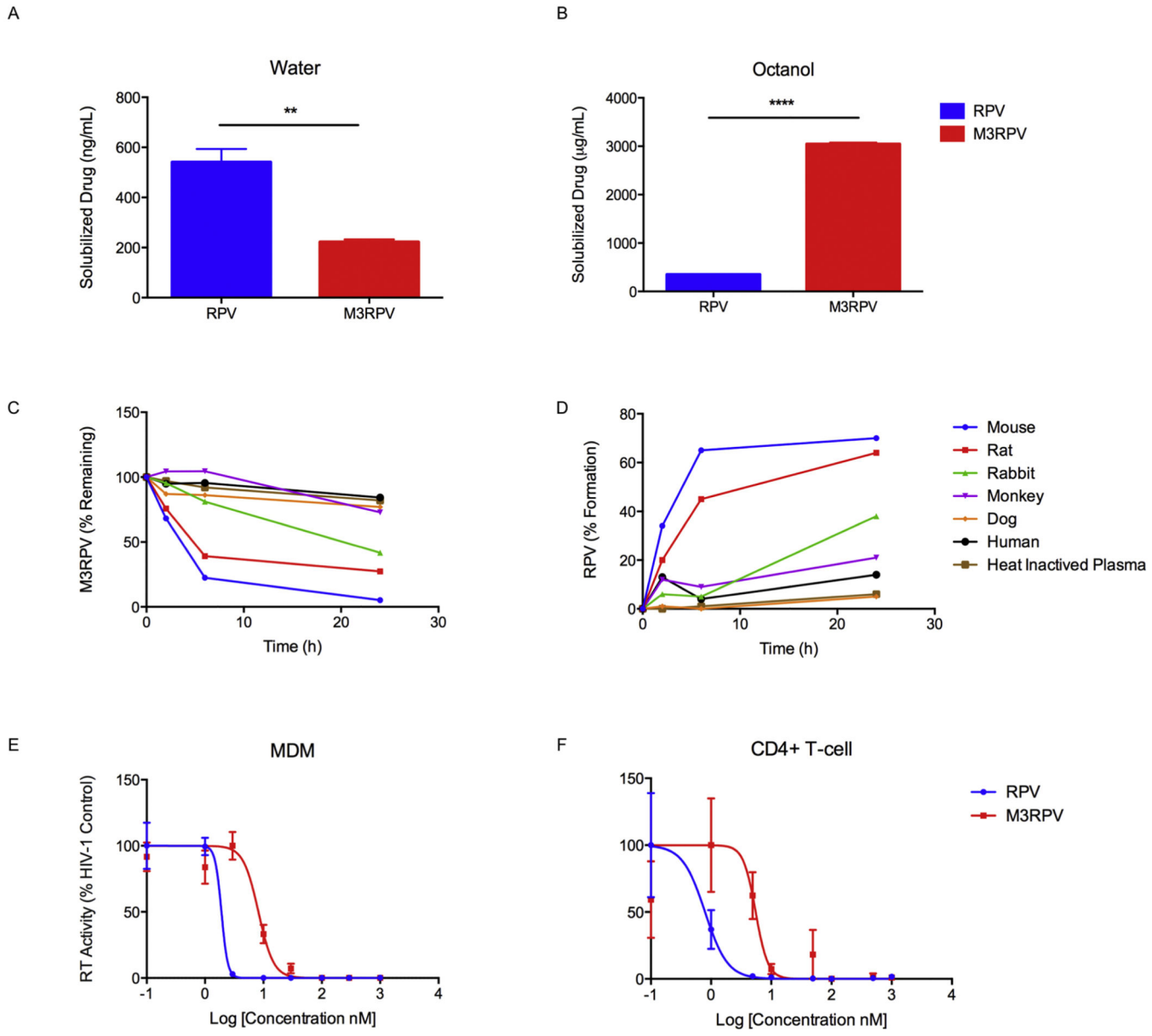

Figure 2. M3RPV characterization.

(A) Water and **(B)** 1-octanol solubility of M3RPV and RPV were measured following 24 hours incubation. Data are expressed as mean ± SEM for n = 3 replicates. (** $P < 0.01$, **** $P < 0.0001$) Plasma cleavage of M3RPV was tested in numerous species (mouse, rat, rabbit, monkey, dog, and human) and **(C)** measured for loss of M3RPV, as well as **(D)** formation of RPV. Antiviral activity of M3RPV and RPV in **(E)** MDM and **(F)** CEM-CD4+ T-cells was investigated at a range of concentrations (0.1–1000 nM) and determined by HIV-1 reverse transcriptase (RT) activity after viral challenge with HIV-1_{ADA} at an MOI of 0.1. Data was normalized and expressed as percentage of HIV-1 control ± SEM; N=3.

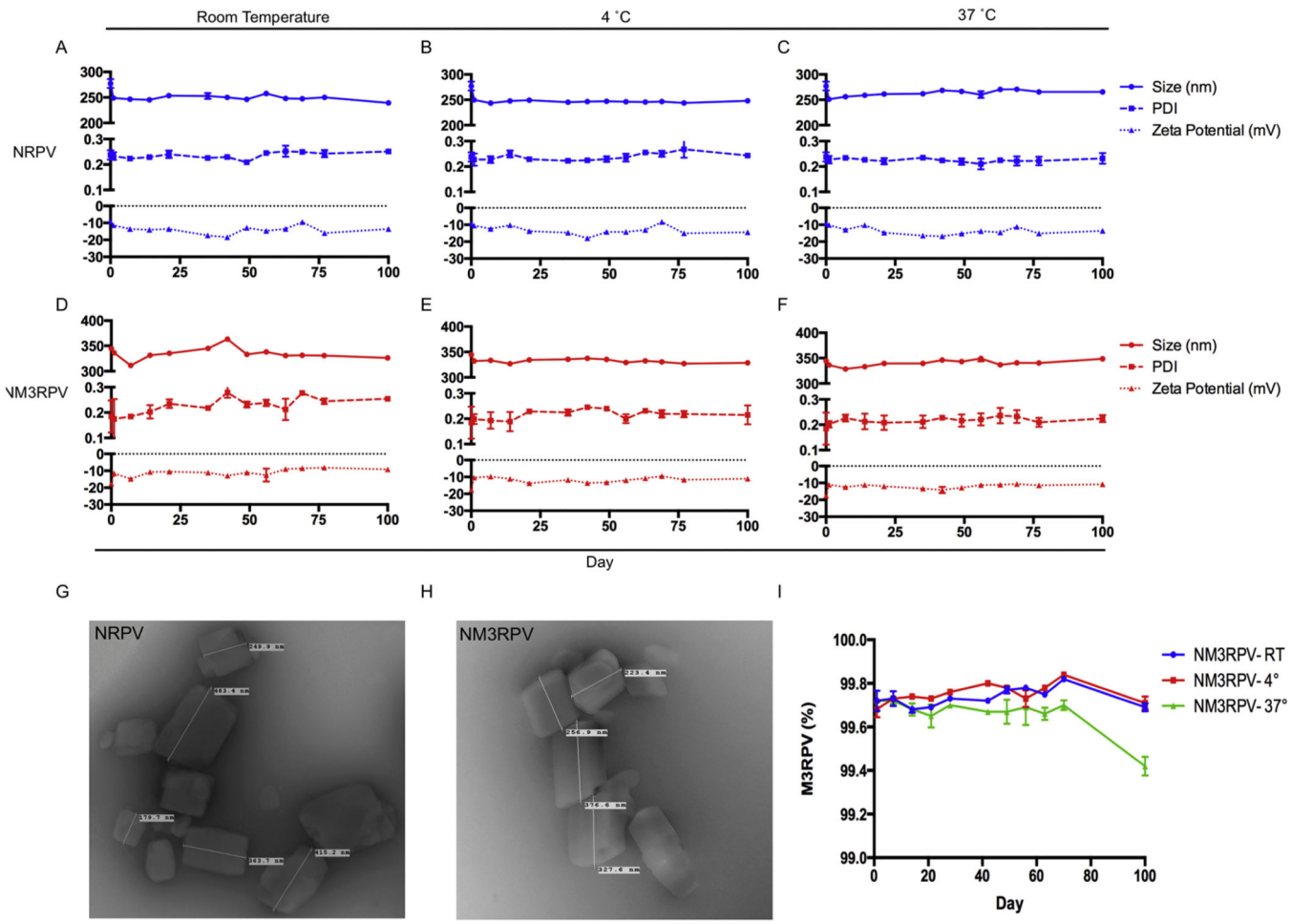

Figure 3. Stability and morphology of NM3RPV and NRPV.

(A-C) Physicochemical stability of NRPV and **(D-F)** NM3RPV were evaluated for size (nm), polydispersity (PDI), and zeta potential (mV) at multiple temperatures (room temperature [(RT],), 4 °C and 37 °C) across 100 days. Data is expressed at mean ± SD for n = 3 measurements. Transmission electron microscopy (TEM) provided a morphological assessment of NRPV **(G)** and NM3RPV **(H)**. **(I)** Prodrug stability within nanoformulated M3RPV was determined by analyzing the ratio of M3PRV to RPV in NM3RPV over a period of 100 days. Data are expressed at mean ± SEM for n = 3 measurements.

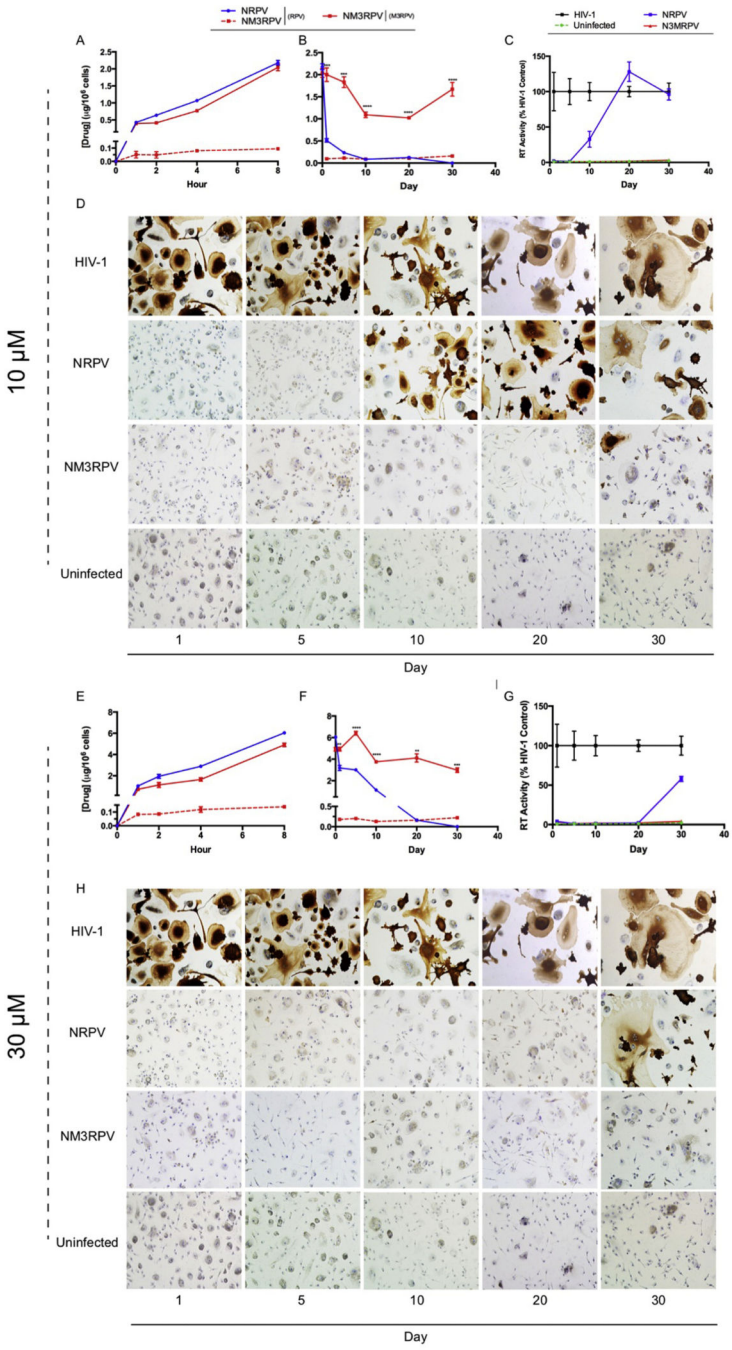

Figure 4. In vitro characterization of NM3RPV in macrophages.

Nanoformulation uptake, retention, and long-term antiretroviral efficacy was assessed in MDMs. Specifically, NM3RPV and NRPV were evaluated for uptake **(A,E)** and retention **(B,F)** of intracellular RPV and M3RPV at concentrations of 10 and 30 μM. Data is expressed as mean ± SEM with n = 3 biological replicates (* $P < 0.05$, ** $P < 0.01$, *** $P < 0.001$, **** $P < 0.0001$ as determined by Student's *t* test). Long-term antiretroviral efficacies of NM3RPV and NRPV were examined after an 8-hour drug treatment with 10 or 30 μM, followed by HIV-1_{ADA} (MOI = 0.1) challenge up to 30 days post treatment.

Infection was characterized by HIV-1 reverse transcriptase (RT) activity **(C,G)** and HIV-1p24 antigen expression **(D,H)**. HIV-1 RT activity was normalized as a percentage of HIV-1 positive control and expressed as mean ± SEM with n = 4 biological replicates. Representative images of MDMs stained for HIV-1p24 antigen expression (brown stain) are shown.

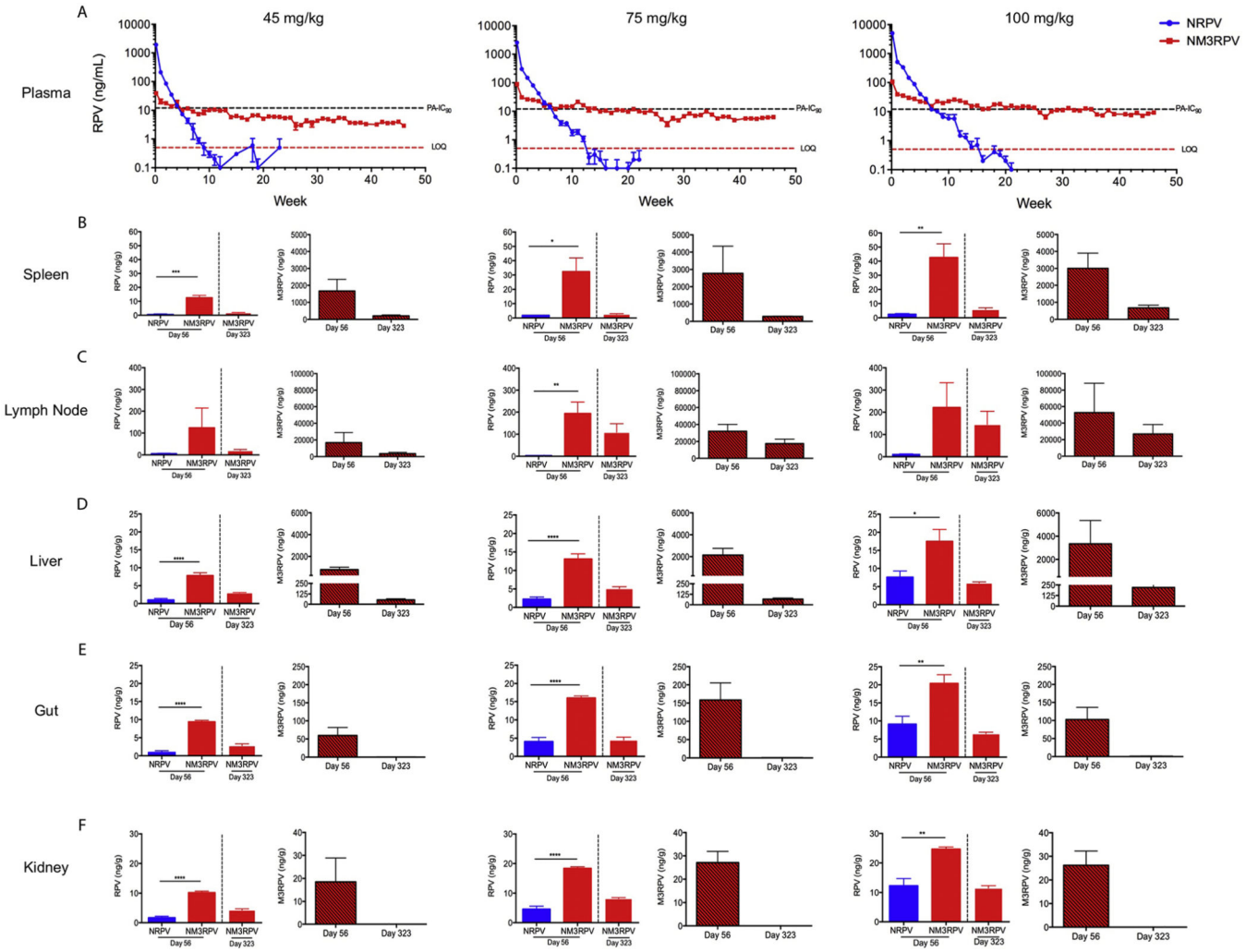

Figure 5. Murine PK and BD.

Male *BALB/cJ* mice were administered a single intramuscular injection of NM3RPV or NRPV at 45, 75, or 100 RPV-eq./kg **(A)** RPV concentrations in plasma were determined at days 1 and 7 then weekly for 46 weeks. PA-IC_{90} and limit of quantitation (LOQ) defined as 12 and 0.5 ng/mL respectively. Tissue biodistribution of RPV and M3RPV was assessed at 56 and 323 days after injection in the **(B)** spleen, **(C)** lymph node, **(D)** liver, **(E)** gut and **(F)** kidney. Data is expressed as mean ± SEM where N = 4/5 biological replicates (**** $P <$ 0.0001, *** $P < 0.001$, ** $P < 0.01$, * $P < 0.05$ by Student's *t* test).

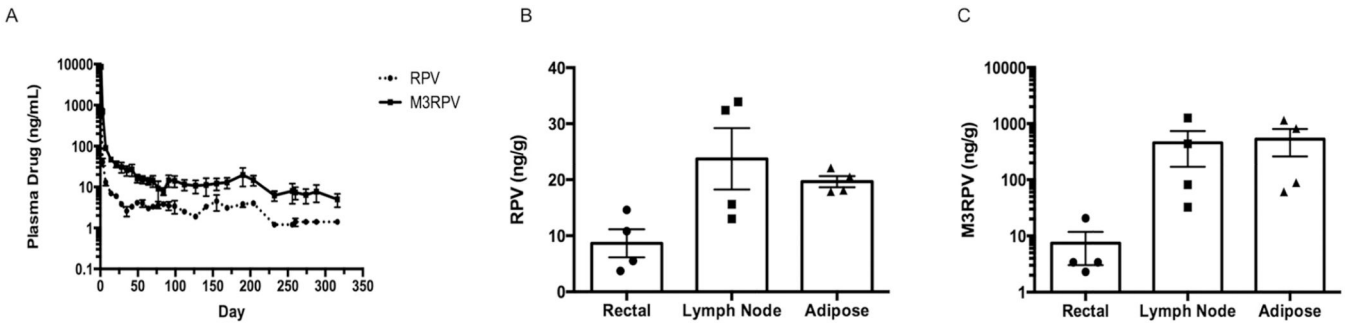

Figure 6. Rhesus macaque PK and BD.

Four rhesus macaques were administered 45 mg/kg RPV-eq. of NM3RPV by a single IM injection. **(A)** Plasma samples were collected and assayed for RPV and NM3RPV at day 1, 7 and weekly throughout the course of study (316 days). Additionally, rectal, lymph node, and adipose tissue biopsies were collected 204 days after drug administration and assayed for RPV **(B)** and NM3RPV **(C)** content. Both plasma and tissue drug concentrations were determined by UPLC-MS/MS. Data are expressed as mean ± SEM for n = 4.